

## Quark-gluon model for diffraction at high energies

Pierre L'Heureux,\* Bernard Margolis, and Pierre Valin

*Physics Department, McGill University, 3600 University Street, Montréal, Québec, Canada H3A 2T8*

(Received 19 April 1985)

We study elastic diffraction in the  $pp$  and  $\bar{p}p$  channels at high energies through an eikonal model, built in impact-parameter space out of QCD and parton-model concepts. The eikonal function is separated into two terms, a constant contribution from valence quarks and a gluon-fusion-initiated term. The latter is responsible for the whole energy dependence of the model at high energies. We discuss the inclusion of a real part for the elastic amplitude, the removal of multiple diffraction zeros, and the behavior of our model up to the multi-TeV energy range (the Froissart bound is not saturated). We find excellent agreement with a large body of experimental data.

### I. INTRODUCTION

The large energy interval between the CERN ISR and the CERN  $\bar{p}p$  Collider ( $S\bar{p}pS$ ) permits us to test the high-energy predictions of various phenomenological models which were developed to study the ISR data. For example, the observed 20% increase in the elastic-to-total-cross-section ratio<sup>1,2</sup> ( $\sigma_{el}/\sigma_{tot}$ ) rules out both a Reggeon-field-theory model,<sup>3</sup> which predicted this ratio to decrease with increasing energy, and the geometrical-scaling (GS) model<sup>4</sup> which predicted it to remain constant. The slower rise of the forward elastic slope<sup>5</sup> compared to that of the total cross section<sup>1</sup> also contradicts GS.

The recent availability of data<sup>6</sup> for the  $\bar{p}p$  channel at the ISR has strengthened theoretical prejudice<sup>7</sup> expecting the disappearance with increasing energy of the crossing-odd amplitude in antiproton-proton collisions, leading eventually to an identical behavior for the  $pp$  and  $\bar{p}p$  channels, according to general asymptotic theorems.<sup>11</sup> We shall adhere to this view here. Under the hypothesis of the existence of a single crossing-even amplitude, some authors<sup>12</sup> have shown that it is possible to fit lower-energy data simultaneously with the newer  $S\bar{p}pS$  results without asymptotically saturating the Froissart bound<sup>13</sup> ( $\sigma_{tot}$  may even become a constant at infinite energy). It therefore does not appear to be necessary, before precise results from higher-energy experiments become available, to build a model explicitly saturating the Froissart bound.

In this paper we study elastic-scattering-related quantities through an eikonal model built in impact-parameter space out of QCD and parton-model concepts. The eikonal function is separated into two components, only one of which bears energy dependence at high energy. We borrow this energy dependence from a model, based on gluon-gluon fusion, for soft nondiffractive inelastic processes in the central region.<sup>14</sup> Our picture (which assumes neither GS characteristics nor an eikonal with factorized energy and impact-parameter dependences) features a rising  $\sigma_{el}/\sigma_{tot}$  ratio, and a forward elastic slope which rises

slower than  $\sigma_{tot}$ ; the latter does not saturate the Froissart bound at extremely high energies. We obtain excellent agreement with a large set of data using only five adjustable parameters, all physically well motivated.

After having constructed our eikonal in Secs. II A and II B, and having compared our model with data in Sec. II C, we briefly discuss two improvements in Sec. III, namely, the inclusion of a proper real part at low energy and the removal of multiple diffraction zeros. Section IV is devoted to discussion and to comments on very-high-energy behavior, while a summary and some concluding remarks appear in Sec. V. Since we do not make any distinction between the  $pp$  and  $\bar{p}p$  channels (except briefly at low energy in Sec. III, and in comparing with data), the word "proton" is generally used but may as well mean "antiproton," in particular in Sec. II A.

### II. THE MODEL

#### A. General framework

Imagine that each of the two colliding protons consists of a collection of partons, each carrying a variable fraction  $x_n$  of the longitudinal momentum of its host proton, and where  $n = 1$  or  $2$  refers to proton No. 1 or No. 2. Assuming that the protons are transversely extended objects in the plane perpendicular to their direction of motion, let  $\mathbf{b}_n$  stand for the variable position vector of each of these partons. Then, let  $G_k(x_n, \mathbf{b}_n)$  be the parton distribution functions, where  $k$  (and, in what follows, also the letters  $i$  and  $j$ ) labels the type of parton (quark  $q$ , antiquark  $\bar{q}$ , or gluon  $g$ ).

The imaginary part of the eikonal function (actually  $2 \text{Im}\chi$ ) is built by adding all elementary inelastic contributions, with cross sections  $\sigma_{ij}(\hat{s}_{ij}(b))$ , from the parton pairs of all types  $ij$  colliding at impact parameter  $b$  ( $b = |\mathbf{b}| = |\mathbf{b}_1 - \mathbf{b}_2|$ ). It incorporates features of both the parton and the geometrical models. We write

$$2\chi(s, b) = i \sum_{ij} \int G_i(x_1, \mathbf{b}_1) G_j(x_2, \mathbf{b}_2) \delta^{(2)}(\mathbf{b}_2 - \mathbf{b}_1 - \mathbf{b}) \frac{\sigma_{ij}(\hat{s}_{ij}(b))}{\sigma_{ij}^0} d^2\mathbf{b}_1 d^2\mathbf{b}_2 dx_1 dx_2, \quad (1)$$

where  $\sigma_{ij}^0$  is a parameter with the same dimensions as  $\sigma_{ij}(\hat{s}_{ij}(b))$  in order to make  $\text{Im}\chi$  dimensionless, and which may have to be fixed differently for each  $ij$ -pair type. The total squared center-of-mass energy is  $s$ , and  $\hat{s}_{ij}(b)$  is the reduced energy of the pair  $ij$ , assumed to depend on  $b$  (see below).

For simplicity, assume that the distribution functions for each type of parton factorize in the  $x_n$  and  $\mathbf{b}_n$  variables

$$G_k(x_n, \mathbf{b}_n) = f_k(x_n) h_k(\mathbf{b}_n) \quad (\text{for all } k). \quad (2)$$

The  $f_k(x_n)$  functions are taken to be the  $x$  distributions of the parton model, used to define the familiar convoluted structure function for pair  $ij$

$$F_{ij}(\tau) = \tau \int_0^1 \int_0^1 f_i(x_1) f_j(x_2) \delta(x_1 x_2 - \tau) dx_1 dx_2, \quad (3)$$

while the  $h_k(\mathbf{b}_n)$  are density profiles entering an analogous definition for a convoluted structure function in impact-parameter space:

$$W_{ij}(b) = \int \int h_i(\mathbf{b}_1) h_j(\mathbf{b}_2) \delta^{(2)}(\mathbf{b}_2 - \mathbf{b}_1 - \mathbf{b}) d^2 \mathbf{b}_1 d^2 \mathbf{b}_2. \quad (4)$$

In order that the density overlaps  $W_{ij}(b)$  represent the normalized effective number of  $ij$ -type pairs at  $b$ , we normalize them to one for head-on collisions, viz.,  $W_{ij}(b=0) = 1$ , for all  $ij$ .

Enforcing the factorization hypothesis of Eq. (2) immediately permits taking a  $W_{ij}(b)$  factor out of the integral in Eq. (1), according to definition (4). Introducing  $1 = \int \delta(x_1 x_2 - \tau) d\tau$ , and using Eq. (3), we obtain

$$\chi(s, b) = \frac{i}{2} \sum_{ij} \frac{W_{ij}(b)}{\sigma_{ij}^0} \int_0^1 F_{ij}(\tau) \sigma_{ij}(\hat{s}_{ij}(b)) \tau^{-1} d\tau, \quad (5)$$

where we assume that  $\hat{s}_{ij}(b) = \tau s W_{ij}(b)$ , i.e., that the subprocess energy depends on the amount of colliding matter for the given  $b$ .

The structure of soft hadron-hadron nondiffractive inelastic events<sup>15</sup> suggests that two terms contribute dominantly to the sum in Eq. (5). Roughly speaking, one can imagine that in these reactions the two groups of valence quarks fly through each other without reacting (or very softly) and produce the leading hadrons, while, upon encounter, the two initial gluon clouds react to yield the bulk of low-transverse-momentum particles in the central region. Equation (5) is thus decomposed as follows.

*First term.* The identical contributions from each of the nine pairs made of a valence quark from each of the two

protons (a valence antiquark in the case of an antiproton) are added together. We attribute  $vv$  subscripts ( $v$  replaces either  $q$  or  $\bar{q}$ ) to all quantities in this term. According to the above rough picture, the valence quarks can interact very softly and, unfortunately, QCD is not useful in this region; we therefore parametrize the whole integral in Eq. (5) as a constant  $\sigma_{vv}$ , to be adjusted by comparing with data. To normalize explicitly this term, we express the dimensionless  $W_{vv}(b)$  in terms of a form factor  $T_{vv}(b)$ , bearing units of inverse cross section, satisfying  $\int T_{vv}(b) d^2 \mathbf{b} = 9$ , and such that  $W_{vv}(b) = T_{vv}(b)/T_{vv}(0)$ . Identifying  $\sigma_{vv}^0 = 9/T_{vv}(0)$ , we replace  $\sum_{vv} W_{vv}(b)/\sigma_{vv}^0$  by  $T_{vv}(b)$  in Eq. (5) and write

$$\chi_V(b) = (i/2) T_{vv}(b) \sigma_{vv}. \quad (6)$$

*Second term.* We put together all reactions initiated by a pair of gluons ( $gg$  subscripts). Since the number of such pairs cannot be determined, we remove the summation symbol and let the parameter  $\sigma_{gg}^0$  fix an effective number to be adjusted later to experimental data. Thus, we have (to simplify the notation, let  $\sigma_{gg}^0 = D^{-1}$ )

$$\chi_G(s, b) = (i/2) D W_{gg}(b) \int_0^1 F_{gg}(\tau) \sigma_{gg}(\hat{s}) \tau^{-1} d\tau, \quad (7)$$

where, from now on,  $\hat{s}$  is short for  $\tau s W_{gg}(b)$ .

The role attributed to two-gluon fusion stems from a scaling law observed by Halzen and collaborators<sup>16</sup> for the production of heavy boson resonances in the central region. If  $\sigma(M)$  is the cross section for producing a particle of mass  $M$  and  $\Gamma$  is its width, it was found that  $M^3 \Gamma^{-1} \sigma(M) \propto F(\tau)$ , where  $F(\tau)$  was an unknown but universal function. Afek, Leroy, Margolis, and Valin<sup>17</sup> revised this scaling law and identified  $F(\tau)$  with  $F_{gg}(\tau)$ , namely, our Eq. (3), calculated from the naive distribution functions

$$f_g(x) = \frac{1}{2} (n+1) x^{-1} (1-x)^n,$$

with the counting-rule value of  $n=5$  (the gluons carry one half of the proton's momentum). Phenomenological evidence that two-gluon fusion may also centrally produce light particles with proper energy dependence and correct normalization for the inclusive single-particle cross sections was given in Ref. 14. The dominant lowest-order QCD process used in that model is  $gg \rightarrow gg$  (the two-step structure of that model is supported by the experimental observation of small direct yield of light particles<sup>15</sup>); we borrow it without modification and identify

$$\sigma_{gg}(\hat{s}) = 9\pi\alpha_s^2(\hat{s}) \{ \delta^{-2} + (\hat{s} + \delta^2)^{-1} [ \frac{17}{12} - \ln(1 + \hat{s}/\delta^2) ] \} \theta(\hat{s} - 4m_{\pi^0}^2),$$

with

$$\alpha_s = 12\pi / [25 \ln(\hat{s}/\Lambda^2)],$$

$$\Lambda = 127 \text{ MeV}, \quad \delta = 0.54 \text{ GeV}.$$

That a state lighter than two  $\pi^0$  mesons cannot be created is accounted for by the  $\theta$  function. The precise form of  $\sigma_{gg}(\hat{s})$  is not critical; in Ref. 17 the process  $gg \rightarrow \bar{q}q$  was used instead of  $gg \rightarrow gg$  and we could still use it to obtain

very similar results to those presented below. This is because elastic scattering is due to the shadow of inelastic events; it does not depend critically on the details of the description for the opening of the inelastic channels, as long as the same overall absorption results, with the appropriate impact-parameter and energy dependences. But the second mechanism offers a better link with the central production of light particles through the model of Ref. 14. It also permits us to use  $n=5$  in  $f_g(x)$  and the renor-

malization group improved  $\alpha_s(\hat{s})$  in  $\sigma_{gg}(\hat{s})$ , instead of  $n=3$  and a constant  $\alpha_s$ , as in Ref. 17.

To summarize, our eikonal has the form

$$\chi(s,b) = \chi_V(b) + \chi_G(s,b), \quad (8)$$

and we neglect any other contribution (from the  $\bar{q}q$  sea, for instance). Note that the first term [given by Eq. (6)] is of the original Chou-Yang type with a factorized eikonal (FE) form,<sup>18-22</sup> but deprived of any energy dependence. The energy dependence is provided by the second term alone [Eq. (7)] and we expect it to become important above the Fermilab energy range. This framework recovers the two-component eikonal model of Afek, Leroy, Margolis, and Valin,<sup>17</sup> except for the  $W_{gg}(b)$  factor in front of the integration over  $\tau$  in  $\chi_G$  which was then chosen to be equal to one. This is an important modification since it will be seen that this gluon-gluon density overlap controls the energy evolution of all the quantities which we intend to study, for instance, the total cross section and the forward elastic slope. The  $\chi_G$  term introduces some scaling effects because of the embedded relation between  $s$  and  $b$ . Our whole eikonal, however, possesses neither recognizable built-in GS nor FE characteristics. It is the interplay between the two terms which will permit us to reproduce the behavior of the data.

Our conventions read

$$\frac{d\sigma}{dt}(s,t) = \pi |f(s,t)|^2,$$

$$\sigma_{\text{tot}}(s) = 4\pi \text{Im}f(s,t=0),$$

$$f(s,t) = i \int_0^\infty (1 - e^{i\chi(s,b)}) J_0(b\sqrt{-t}) b db.$$

### B. A simple version of the model

Since the parton model provides no information on the  $h_k(\mathbf{b}_n)$  of Eq. (4), we use the Chou-Yang picture<sup>18,19</sup> and take  $T_{vv}(b)$  to resemble the Fourier-Bessel transform of the proton's electromagnetic form factor squared. Using a dipole approximation to the form factor, one gets

$$T_{vv}(b) = (3\mu^2/32\pi)(\mu b)^3 K_3(\mu b), \quad (9)$$

where  $K_3(z)$  is a modified Bessel function and  $\mu$  is a parameter that will be left adjustable to account for eventual small differences between the charge and valence matter distributions inside the proton.

For simplicity, and in the absence of any precise theoretical guideline, we use the same shape for the gluons, but normalized to one at  $b=0$ , and with a possibly different parameter  $\mu'$ . We take then

$$W_{gg}(b) = \frac{1}{8}(\mu'b)^3 K_3(\mu'b). \quad (10)$$

The quantities  $\mu^{-1}$  and  $\mu'^{-1}$  characterize the ranges of quark-quark and gluon-gluon interactions in  $b$  space. Intuitively we expect  $\mu \simeq \mu_{\text{em}}$ , and  $\mu' < \mu$  since the gluons should presumably provide confinement and screening for the colored quarks and thus have a larger range.

Compared with Ref. 17, where  $\chi_G$  had a very long tail at large values of  $b$  which caused a very rapid increase in  $\sigma_{\text{tot}}$  above the ISR, the desirable asymptotic  $\sigma_{\text{tot}} \propto \log^2 s$

rise and, unfortunately, a less desirable Carrigan-type break in  $d\sigma/dt$  at small  $|t|$  at the  $S\bar{p}pS$ , it is remarkable that the introduction in Eq. (7) of  $W_{gg}(b)$  with a single new parameter permits us to reproduce the flatter trend of the new data very well. The proton is now pictured as a more compact object whose shape is built of two similar distributions with different ranges.

Up to now our description is only valid at high energies ( $\sqrt{s} \gtrsim 60$  GeV). A very simple way to parametrize the lower-energy behavior of  $\sigma_{\text{tot}}$  ( $6 \lesssim \sqrt{s} \lesssim 60$  GeV) is to modify  $\chi_V$  from Eq. (6) to<sup>17</sup>

$$\chi_V(s,b) = (i/2)(1 + C/\sqrt{s})T_{vv}(b)\sigma_{vv}. \quad (11)$$

This simulation of effects due to Regge exchanges completes the formulation of the imaginary part of  $\chi$  for this simple version of the model. The models seeking to reproduce the features of  $d\sigma/dt$  at ISR energies can do well without including a real part for the elastic amplitude since the real part is generally unimportant except for the filling of the first diffraction zero. At higher energies however, like at the  $S\bar{p}pS$ , the real part is believed to be significant enough to produce the transformation of the dip into the observed shoulder; the implementation of a real part then becomes necessary to achieve a fit to the data.

In what follows, we generate a real part for the  $\chi_G$  term from the substitution<sup>23,24</sup>

$$s \rightarrow s e^{-i\pi/2}, \quad (12)$$

valid for an even amplitude and equivalent to the use of a derivative analyticity relation.<sup>25</sup> But it would be improper to apply Eq. (12) to  $\chi_V$  in Eq. (11) because it would automatically impose crossing-even symmetry to a term meant to parametrize contributions from low-energy Regge amplitudes. Since a proper Regge term would be built from both even and odd amplitudes, and since Eq. (12) can only provide us with an even real contribution, the real part obtained in the low-energy region would inevitably be incorrect.

The most important feature which we want to put in evidence is our high-energy model for  $\chi_G$ ; the low-energy parametrization  $C/\sqrt{s}$  in  $\chi_V$  is merely a convenience to extend the applicability of the overall picture but not an essential feature. Since it is extremely simple and it permits us to reproduce a wide range of data by adjusting a minimal number of parameters, we thus propose the following temporary simplifying procedure: we free ourselves of calculating a real part in the ISR energy range where the  $C/\sqrt{s}$  term still contributes and only compute it above  $\sqrt{s} \simeq 250$  GeV where  $C/\sqrt{s}$  is negligible and where the real part is an essential ingredient in the evaluation of  $d\sigma/dt$ .

In Sec. IIC we determine the five physically well-motivated parameters,  $\sigma_{vv}$ ,  $\mu$ , and  $C$  in  $\chi_V$  of Eq. (11),  $\mu'$  and  $D$  in  $\chi_G$  of Eq. (7), and compare the predictions of our model with various experimental quantities.

In Sec. III, in order to improve our picture in its finer details, we show how it is possible to introduce a better Regge parametrization which permits us to distinguish the  $\bar{p}p$  from the  $pp$  case at low energy and to provide an

acceptable real part. We also modify the form factor  $T_{vv}$  to remove the multiple diffraction zeros in the imaginary part of the amplitude resulting unavoidably<sup>26,27</sup> from the chosen dipole form factor leading to Eq. (9).

### C. Calculations and results

We have made a simultaneous fit of  $\sigma_{\text{tot}}$  and  $B(0)$  for  $6 \leq \sqrt{s} \leq 546$  GeV and of  $d\sigma/dt$  at  $\sqrt{s} = 30.7, 52.8,$  and  $546$  GeV. The parameter values listed in Table I do not necessarily constitute the "best" fit one could obtain although they should be close to it. At the  $S\bar{p}pS$ , where according to the previous discussion this procedure is legitimate, the real part of the elastic-scattering amplitude is

generated from the substitution (12). The obtained value of  $\sigma_{vv}$  accounts for an asymptotic valence-quark contribution of the correct magnitude of  $9 \times 3.06 \approx 27$  mb in the inelastic cross section. In qualitative agreement with our intuitive expectations we find  $\mu' < \mu$ , with  $\mu$  reasonably close to the electromagnetic-form-factor value of 0.843 GeV.

In all the figures which we now present, the results of this simple version (version 1) are drawn as solid curves. The first three figures show  $d\sigma/dt$  at various energies and for various regions of  $|t|$ ; the curves at the energies not used in the fit are calculated from the resulting parameters. The agreement with the data is quite good. A single notable disagreement occurs in Fig. 1 over the range  $0.5 \leq |t| \leq 1.0$  GeV<sup>2</sup> at  $\sqrt{s} = 44.7$  GeV. We plot the data from the overall analysis of Amaldi and Schubert<sup>28</sup> and compiled by Schubert in Ref. 29. We are reluctant to consider this discrepancy to be significant because Valin<sup>30</sup> has shown, using unitarity bounds, that there were questionable points in the ISR data at certain energies. Unfortunately the energy  $\sqrt{s} = 44.7$  GeV was not studied in Ref. 30. The bound is a particularly powerful tool when used to verify the consistency of normalization among ad-

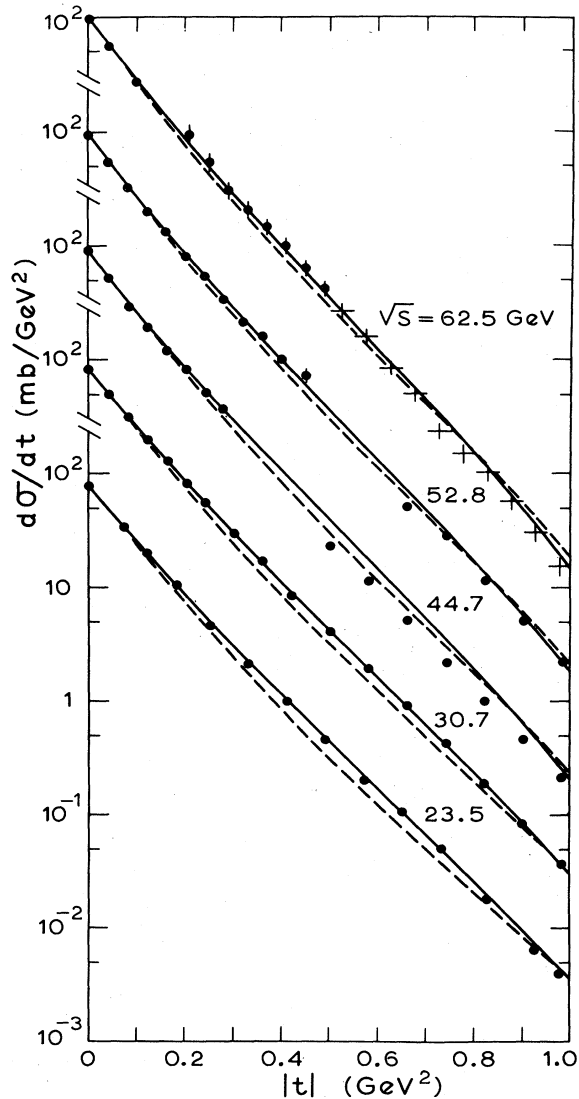


FIG. 1. Elastic differential cross section at small and medium  $|t|$  for  $pp$  at the five ISR energies. Data points are from the compilation of Ref. 29. Solid curves represent version 1 of the model; short-dashed curves are for version 3.

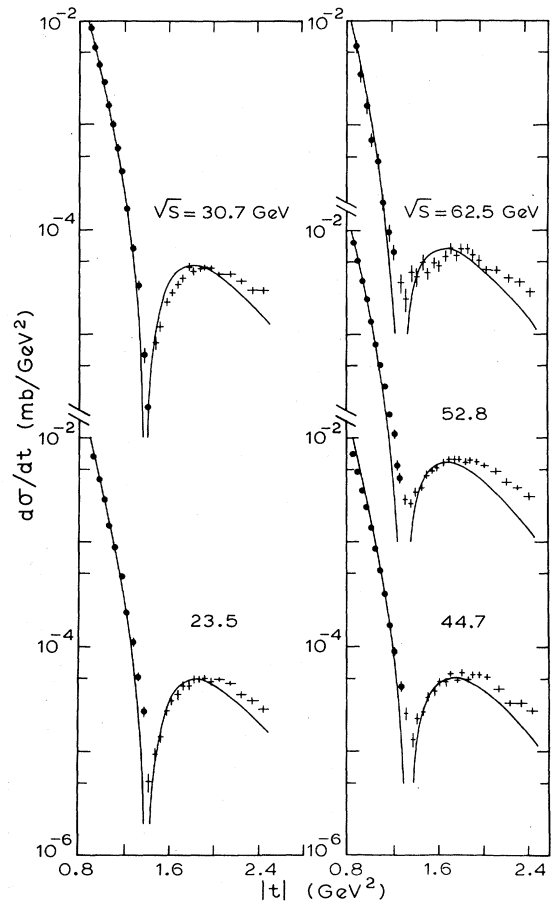


FIG. 2. Elastic differential cross section at large- $|t|$  values for  $pp$  at the five ISR energies. Data points are from Ref. 29. Only version 1 is plotted here; there is no real part.

TABLE I. Values of the parameters resulting from fits to some part of the data for each of the three versions of the model. Version 1 has five adjustable parameters, version 2 has seven and, for simplicity, out of the nine parameters of version 3 only four were allowed to vary, the five others being directly taken from those of version 2.

Parameter	Version 1	Version 2	Version 3
$\sigma_w$ (mb)	3.0585	3.8005	3.6700
$D$ (GeV <sup>2</sup> )	$1.2695 \times 10^{-4}$	$1.0372 \times 10^{-4}$	$1.0372 \times 10^{-4}$
$\mu'$ (GeV)	0.64131	0.63432	0.63432
$\mu$ (GeV)	0.93753	0.91721	
$\gamma$ (GeV)			2.2391
$m_1$ (GeV)			0.67544
$m_2$ (GeV)			1.8987
$C$ (GeV)	5.3315		
$\beta_+$		19.713	19.713
$\beta_-$		6.2100	6.2100
$a$ (GeV <sup>-2</sup> )		0.94318	0.94318

acent data points; the absence of adjacent points for  $|t| < 0.5$  GeV<sup>2</sup> prevents the reaching of a clear conclusion.

In Fig. 2, unfilled diffraction zeros are unavoidable because of our neglect of a real part, as is the presence of other zeros (not shown) artificially generated by Eq. (9).<sup>26,27</sup> A real part is included in Fig. 3 which illustrates

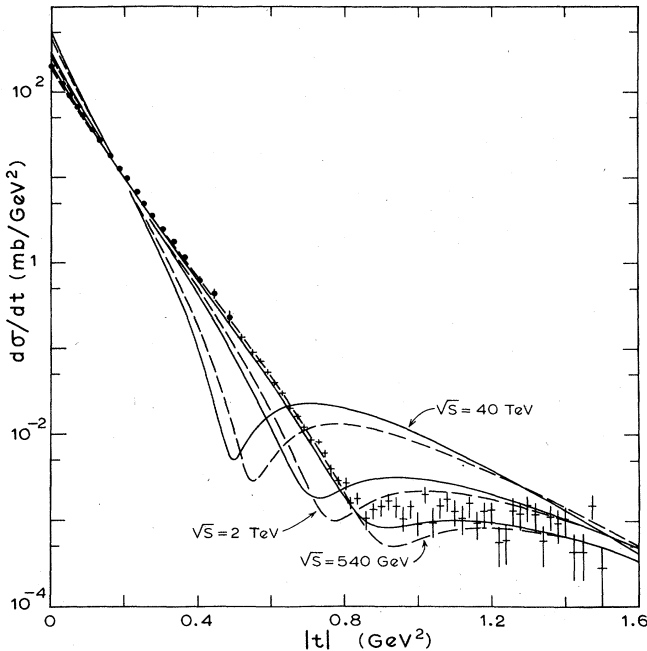


FIG. 3. Elastic differential cross section for  $\bar{p}p$  (or  $pp$ ; they are not distinguished at high energies in our model). The model is compared with data from Refs. 5 and 31 at the  $S\bar{p}pS$ . Also shown are predictions for the Fermilab Tevatron and the Superconducting Super Collider. Solid curves, version 1; long-dashed curves, version 2.

higher-energy predictions. With increasing energy a dip is gradually recovered as the first zero of the imaginary part moves inward.

In line with previous comments,  $\rho(0)$  is calculated only above  $\sqrt{s} \simeq 250$  GeV and shown in Fig. 4 together with the fits to  $\sigma_{\text{tot}}$  and  $B(0)$  at all energies. The regular behavior (no Carrigan-type break) of the local slope

$$B(t) = (d/dt)[\ln(d\sigma/dt)]$$

is compared with  $S\bar{p}pS$  results in Fig. 5(a).

Most models which reproduce well the evolution of elastic differential cross sections from the ISR to the  $S\bar{p}pS$  possess (or nearly possess) factorized eikonal characteristics.<sup>18-22</sup> From the approximate relation

$$\sigma_{\text{el}}/\sigma_{\text{tot}} \simeq [1 + \rho^2(0)]\sigma_{\text{tot}}/16\pi B(0), \quad (13)$$

which is exact for a purely exponential  $d\sigma/dt$  and a  $t$ -independent  $\rho$ , it is obvious that any model which reproduces both  $\sigma_{\text{tot}}$  and  $B(0)$  reasonably well at the  $S\bar{p}pS$  also predicts a good  $\sigma_{\text{el}}/\sigma_{\text{tot}}$  ratio, considering the experimental errors; see Fig. 5(b). Figure 5(a) shows that  $d\sigma/dt$  is not purely exponential at small  $|t|$  in our model (as in most), but it is still possible to use Eq. (13) in heuristic arguments for the purpose of comparison between various FE models or between various parameter sets within a given model, if we choose an effective or average value of  $B(t)$  at small  $|t|$  to put in Eq. (13). Choosing the value at  $|t| = 0.06$  GeV<sup>2</sup> works well at the  $S\bar{p}pS$  energy.

On the other hand, the energy evolution in  $b$  space of the inelastic overlap function

$$G_{\text{in}}(s, b) = 1 - e^{-2\text{Im}\chi(s, b)}$$

is a more stringent test. Over the ISR energy range

$$\Delta G_{\text{ISR}} = G_{\text{in}}(s = (62.5 \text{ GeV})^2, b) - G_{\text{in}}((23.5)^2, b),$$

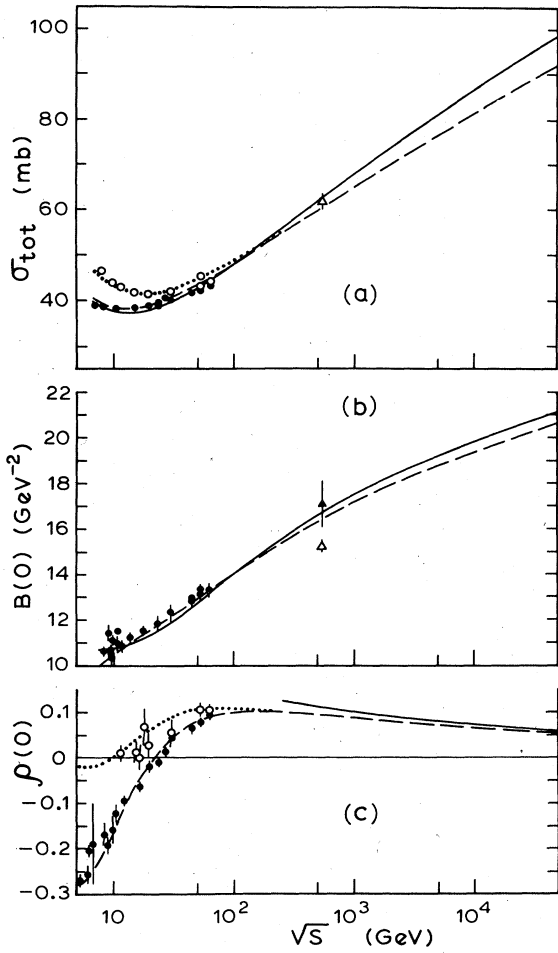


FIG. 4. Three forward quantities. In all cases solid curves are version 1, long-dashed curves version 2. Dotted curves are for the  $\bar{p}p$  case (at low energy) of version 2. Data are a selection of points from the following references: Refs. 28 and 29 ( $pp$ , solid circles); Refs. 6, 10, and 32–34 ( $\bar{p}p$ , open circles); Refs. 1 and 5 ( $\bar{p}p$ , UA4, open triangles); Ref. 2 ( $\bar{p}p$ , UA1, solid triangle). (a) Total cross section. (b) Forward elastic slope (indistinguishable in our model for the  $pp$  and  $\bar{p}p$  cases at low energy—see Sec. III B). (c) Forward ratio of real to imaginary parts of the elastic amplitude; note that for version 1 it is calculated only at high energies—see Secs. II B, II C.

plotted in Fig. 6, it is consistent both in magnitude and in shape with the Amaldi-Schubert<sup>28</sup> result extracted from the differential-cross-section data, except that at  $b=0$  we have  $\Delta G_{\text{ISR}} \neq 0$ , indicating a departure from pure GS. For the energy interval from the ISR to the  $S\bar{p}pS$ , we also plot in Fig. 6

$$\Delta G_{\text{SPS-ISR}} = G_{\text{in}}(s=(546 \text{ GeV})^2, b) - G_{\text{in}}((52.8)^2, b),$$

and obtain good agreement with the BEL (blackier-edgier-larger) behavior discussed by Henzi and Valin<sup>35</sup> (accounting for the fact that at the time they took a higher value for  $\sigma_{\text{tot}}$  than the current one).

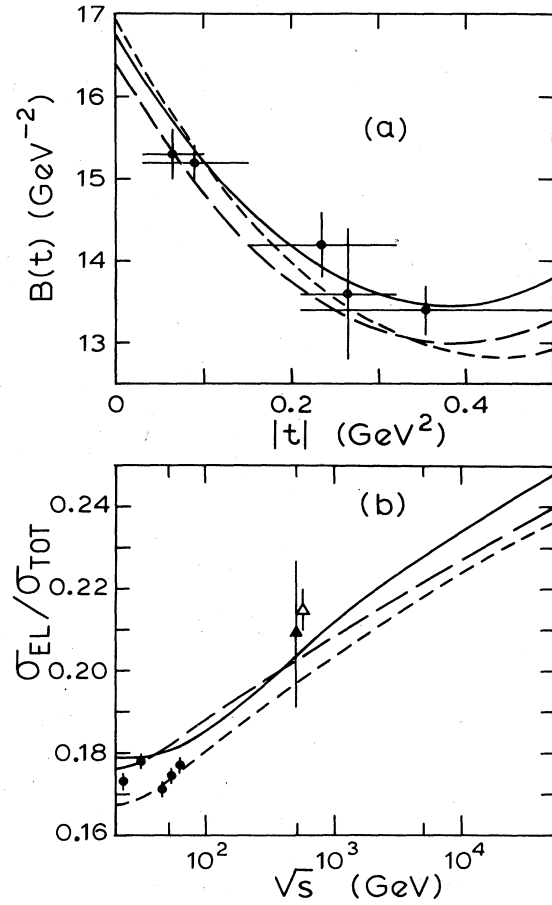


FIG. 5. In both cases shown, solid curve is version 1, long dashed curve is version 2, and short-dashed curve is version 3. (a) Local elastic slope at the  $S\bar{p}pS$  as a function of  $|t|$ ; data from Ref. 5. (b) Ratio of elastic to total cross section as a function of energy; solid circles are  $pp$  data from Ref. 28; open and solid triangles are  $\bar{p}p$  data from the UA4 (Ref. 1) and the UA1 (Ref. 2) collaborations, respectively.

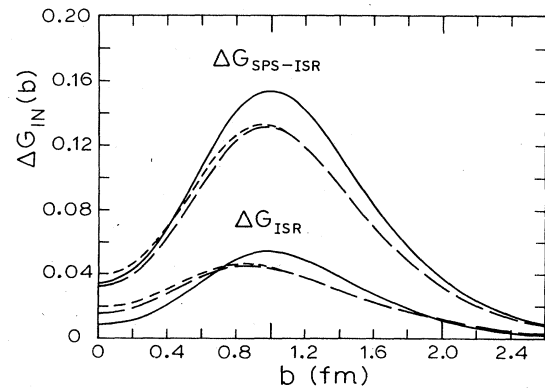


FIG. 6. Differences in inelastic overlap functions. Lower curves show  $\Delta G_{\text{ISR}}$ , the difference in  $G_{\text{in}}(s, b)$  between  $\sqrt{s}=62.5$  and  $23.5$  GeV. Upper curves show  $\Delta G_{\text{SPS-ISR}}$ , the same quantity but between  $\sqrt{s}=546$  and  $52.8$  GeV. Curve convention as in Fig. 5.

### III. REFINEMENTS OF THE MODEL

#### A. The real part at the ISR

The difficulty of including a real part for the elastic amplitude in a precise manner because of our simplified Regge term, is a drawback of version 1. Borrowing a proven Regge parametrization by Chiu<sup>36</sup> to replace our own is the shortest path toward a remedy. Chiu takes (including an  $E^{-1}$  kinematic factor;  $E \approx s/2m_p$ )

$$\begin{aligned} \tilde{R}(s,t) = & -\beta_+ e^{a+t} (e^{-i\pi\alpha_+} + 1) E^{\alpha_+ - 1} \\ & + \xi \beta_- e^{a-t} (e^{-i\pi\alpha_-} - 1) E^{\alpha_- - 1}, \end{aligned} \quad (14)$$

where the  $pp$  and  $\bar{p}p$  channels are distinguished by choosing  $\xi = +1$  or  $\xi = -1$ , respectively. Reference 36 uses exchange-degenerate slopes  $a_+ = a_- = a$  and standard trajectories  $\alpha_{\pm} = \frac{1}{2} + t$  (contrast Refs. 20 and 21).

Transforming to  $b$  space and introducing the eikonal approximation (to incorporate multiple-scattering effects), Eq. (8) is replaced by a three-component eikonal

$$\chi(s,b) = R(s,b) + \chi_V(b) + \chi_G(s,b). \quad (15)$$

The  $R$  term decreases with increasing energy,  $\chi_V$  has now no  $s$  dependence [ $C=0$ , we recover Eq. (6)], and  $\chi_G$  is unchanged. Consequently,  $C$  is replaced by three new parameters  $a$ ,  $\beta_+$ ,  $\beta_-$ , and  $R(s,b)$  includes an appropriate real part stemming from both even and odd contributions; the real part of  $\chi_G$  comes from the substitution (12) as before.

We simultaneously fit the seven parameters of this second version (version 2) to the same data set as before with some values of  $\rho(0)$  added. Again no detailed fit was attempted; no  $\bar{p}p$  data points for low-energy  $\rho(0)$  or  $\sigma_{\text{tot}}$  were included either—only  $pp$ . The  $\bar{p}p$  curves shown in Fig. 4 (we discuss the results in Sec. III B) were calculated *a posteriori* through the change of sign of  $\xi$  in Eq. (14) and from the fitted parameters listed in Table I.

#### B. Removal of multiple diffraction zeros

We shall borrow once again a proven solution, this time to remove the multiple diffraction zeros. We replace the dipole form factor squared leading to Eq. (9) by the expression of Bourrely, Soffer, and Wu,<sup>20,21</sup>

$$\tilde{T}_{vv}(t) = [(1-t/m_1^2)(1-t/m_2^2)]^{-2} (\gamma^2 + t) / (\gamma^2 - t), \quad (16)$$

namely, a double pole squared times a function which we shall call the BSW factor. This factor was an *ad hoc* introduction by these authors in order to reproduce the ISR differential cross-section data at large  $|t|$ ; the need for it is suggested by the work of Franco.<sup>37</sup> We add the  $b$ -space inversions of Eqs. (14) and (16) to Eq. (7) and build a three-component eikonal as in Eq. (15). Ignoring the Regge term for the moment, we recall that our two-component eikonal for the Pomeron receives contributions from a constant valence-quark structure (now with a modified form factor) and from a cloud of gluons which provides the whole energy dependence at high energies.

Our approach is to be contrasted with two recent single-component eikonal models, described in the next paragraph, which have a structure similar to that of Eq. (16).

Sanielevici and Valin have proposed an interpretation of the BSW factor as a reduced normalized valon-valon scattering amplitude, approximately universal for all hadrons.<sup>38</sup> Part of the energy evolution effects must be lumped into  $\gamma$ , but no theoretical prediction for the shape of  $\gamma(s)$  can be given *a priori*; it has to be phenomenologically determined from data.<sup>39</sup> In their model, the role of our double pole is played by the contribution of structureless valons in the host hadrons. In a similar approach, Glauber and Velasco,<sup>40</sup> instead of a double pole, use two different and detailed parametrizations for the proton form factor. They also examine two forms for the extra  $t$  dependence, neither of which is the BSW factor. This extra  $t$  dependence is interpreted as being due to a parton-parton interaction range of roughly half a fermi. They comment only very briefly on energy dependence.

We now return to the discussion of our own model in which the parameter  $\gamma$  in Eq. (16) will remain energy independent, as in Refs. 20 and 21. This third version (version 3) is identical to version 2 except for the form factor change. To shorten the numerical exercise we freeze five out of the nine parameters to their version 2 values. Only  $\sigma_{vv}$ ,  $\gamma$ ,  $m_1$ , and  $m_2$  are left adjustable, the last three replacing  $\mu$  of versions 1 and 2. We perform the fit on  $\sigma_{\text{tot}}$ ,  $B(0)$ ,  $\rho(0)$ , and at a single energy for  $d\sigma/dt$ :  $\sqrt{s} = 52.8$  GeV. The calculations for  $d\sigma/dt$  at other ISR energies are made from the resulting parameters, listed in Table I.

We only plot in the figures results from versions 2 (long-dashed curves) and 3 (short-dashed curves) which are either new or sufficiently different from those of version 1 to be discernible. In Figs. 3, 4(a), and 4(c), the model calculations with the chosen parameters are virtually identical for versions 2 and 3, and only those of version 2 are plotted. The results shown are slightly different from those of version 1. We could have forced the fit to recover nearly the same curves as before but preferred to exhibit the results like this as we can then illustrate typical "bands of predictions" and this is equivalent to showing the behavior of the model under small parameter variations within each of the given versions. Figure 4(c) is a new result,  $\rho(0)$  now being correctly calculable at lower energies.

In Fig. 1, the calculated elastic differential cross sections from version 2 at the ISR are very similar to those of version 1 (but slightly different at the two lowest energies) and not plotted. Because of our simplified numerical procedure, version 3 has a less convincing  $d\sigma/dt$  in the medium- $|t|$  range at the two lowest ISR energies in comparison with version 1, as can be seen in Fig. 1. We nonetheless plot these worst cases since there is little doubt that, by working out a minimization simultaneously on all the ISR data and on the full nine-parameter space, one could improve the picture slightly. We do not pursue this further because the use of Eq. (16) as it stands seems doomed to generate imperfect results. As did the authors of Refs. 20 and 21, we used a value of  $m_1$  around 0.6 GeV which is convenient to reproduce the electromagnetic form factor but, on the other hand, is inherently suscepti-

ble to create some problems in the medium- $|t|$  range, because it generates a too low opacity at  $b=0$  at the ISR. Better agreement in this  $|t|$  region could presumably be obtained through the use of more detailed proton form factors, like those used for example by Glauber and Velasco.<sup>40</sup>

Figure 7 shows how version 2 is unsatisfactory in the dip region at the ISR (modifying only the Regge term produces a dip which is too filled and which varies too rapidly with the energy), and how the form factor of version 3 permits us to restore a proper dip and remove the second diffraction zero simultaneously. The agreement with experiment at large  $|t|$  is quite good except at  $\sqrt{s}=23.5$  GeV, where the second maximum is off by a factor of 2.

As for large  $|t|$ , we do not show in Fig. 3 any prediction for  $|t| \geq 1.6$  GeV<sup>2</sup>, because we directly inherit from Eq. (16) almost the same large- $|t|$  behavior as that of Ref. 21. It should be mentioned that  $d\sigma/dt$ , at  $\sqrt{s}=2$  TeV, for example, crosses below the ISR  $d\sigma/dt$  somewhere between  $|t|=2.0$  and  $3.0$  GeV<sup>2</sup>; the precise location of the crossover point of course depends on the chosen ISR energy. Sanielevici and Valin, in the framework of their single-component eikonal model,<sup>39</sup> have shown that it is possible to remove that early crossover in  $d\sigma/dt$  at energies above the ISR in a manner similar to that produced by the BEL parametrization of the short-range expansion for  $G_{in}$  of Henzi and Valin,<sup>41,42</sup> by the introduction of the energy dependence for  $\gamma$  mentioned above. Eventual modifications could be made to our model, should future experiments indicate a need for them.

Because of the assumed exchange degeneracy in  $R(s,b)$ , the forward slopes in versions 2 and 3 cannot be distinguished between the  $pp$  and the  $\bar{p}p$  cases at low energy [Fig. 4(b)]. The numerous complications required to achieve such a distinction (see, for example, Ref. 9) were left aside. In version 2,  $B(t)$  [Fig. 5(a)] preserves the shape of version 1, but is shifted downward by approximately  $0.4$  GeV<sup>-2</sup>; this is understandable at  $|t|=0.06$  GeV<sup>2</sup> through Eq. (13). The use of Eq. (16) in version 3 leads (also because of small  $m_1$ ) to a more peaked forward  $d\sigma/dt$ . In fact  $B(0)$  (not shown) would be about  $1.0$  GeV<sup>-2</sup> above the ISR data in Fig. 4(b).

In Fig. 6,  $\Delta G_{\text{SPS-ISR}}$  suffers only a normalization change reflecting the small difference in the behavior of  $\sigma_{\text{tot}}$  compared with version 1. The fact that  $\Delta G_{\text{ISR}}$  is computed between the highest and the lowest ISR energies and that the latter is less well reproduced by versions 2 and 3 than by version 1 explains the modification in its shape.

It is only recently that  $\bar{p}p$  data for the medium- $|t|$  range at the ISR has become available. In the interval  $0.1 \lesssim |t| \lesssim 1.0$  GeV<sup>2</sup> there seems to be no significant differences with the  $pp$  channel at  $\sqrt{s}=31, 53,$  and  $62$  GeV (Refs. 43 and 44). At  $\sqrt{s}=53$  GeV, in the region which corresponds to the location of the dip and second maximum in  $pp$ ,  $1.0 \lesssim |t| \lesssim 2.1$  GeV<sup>2</sup>, it is seen in Refs. 44 and 45 that only the points of  $\bar{p}p$  belonging to the dip itself lie above the  $pp$  data. The model of Islam and collaborators<sup>46</sup> predicts a dip in  $\bar{p}p$  at  $|t|=1.0$  GeV<sup>2</sup> and is in

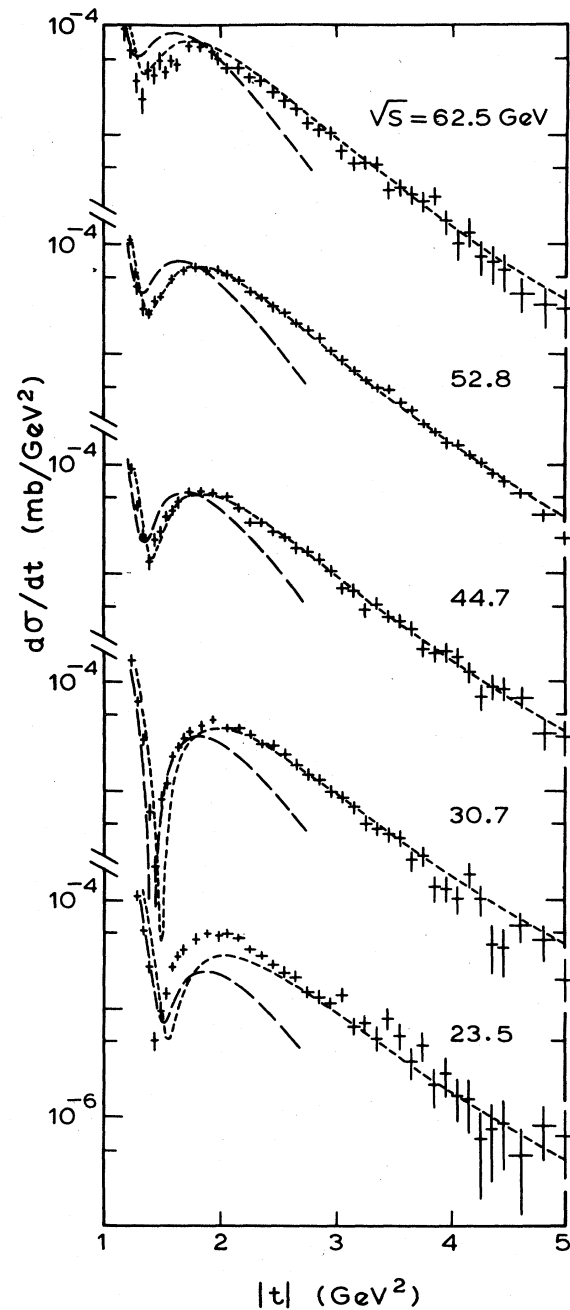


FIG. 7. Large- $|t|$  behavior of  $pp$  elastic differential cross section at the ISR for versions 2 and 3 (long and short dashes, respectively). Data from Ref. 29.

disagreement with the data. The model of Donnachie and Landshoff<sup>47</sup> reproduces well the shape of the  $\bar{p}p$  data, but lies above it for  $|t| \geq 1.0$  GeV<sup>2</sup>. Contrary to these models, our version 3 predicts only a very small difference between the  $pp$  and  $\bar{p}p$  channels and is thus in general agreement with these recent data, except for the apparently shallower dip of  $\bar{p}p$ .



#### IV. DISCUSSION

Whereas a simple calculation reveals that in the model of Ref. 17  $\sigma_{\text{tot}}$  grows asymptotically as  $\log^2 s$ , and saturates the Froissart bound, here the presence of  $W_{gg}(b)$ , the second form factor, makes it almost impossible<sup>48</sup> to deduce analytically the ultimate behavior of  $\sigma_{\text{tot}}$  (the analysis would be similar in spirit to that of Ref. 27). One must instead rely on the numerical results of the complete calculation to see the trend, as in Fig. 4, where we consider the TeV range as the highest energy region of practical interest. The real asymptotic regime of our model is so slowly established as to be beyond the reach of any conceivable accelerator and is therefore only of academic interest. The power  $\beta$ , calculated locally in a parametrization of the form  $\sigma_{\text{tot}} \propto \log^\beta s$ , smoothly decreases from about two at the ISR to about one at the  $S\bar{p}pS$ , and keeps decreasing up to above  $\sqrt{s} = 50$  TeV. It is indeed seen in Fig. 4(a) that  $\sigma_{\text{tot}}$  grows roughly as  $\log s$  in a small energy interval around the  $S\bar{p}pS$  region and exhibits a slow flattening at higher energies.

Our overall high-energy behavior is similar to that of Bourrely and Martin and of Block and Cahn<sup>12</sup> which fit data up to the  $S\bar{p}pS$ ,<sup>49</sup> and which lead eventually, in their case, to a constant  $\sigma_{\text{tot}}$ ; we also share with them a maximal value of  $\rho(0)$  of about 0.10–0.11 at about  $\sqrt{s} = 300$  GeV. The slower rise of  $B(0)$  with  $s$  compared with that of  $\sigma_{\text{tot}}$  in our picture is readily understood through Eq. (13), considering that all FE-type models (and our model possesses some characteristics of an FE model at high energies) predict an asymptotic value of  $\sigma_{\text{el}}/\sigma_{\text{tot}} = \frac{1}{2}$ . This ratio thus has to increase from its  $S\bar{p}pS$  value in order to approach  $\frac{1}{2}$  in going toward the TeV range and consequently  $B(0)$  rises progressively slower than  $\sigma_{\text{tot}}$ .

The work presented here and that of Ref. 17 most significantly differ in the presence of  $W_{gg}(b)$  in Eq. (17) and each illustrates a quite different behavior for  $\sigma_{\text{tot}}$  [without the  $W_{gg}(b)$  factor the rise is much faster]. Our arbitrary but simple hypothesis for the shape of  $W_{gg}(b)$  in Eq. (10) has proven to be perfectly appropriate to describe the available data, but another choice could be made in order to obtain a different behavior for the total cross section. As in the instance where only large- $|t|$  measurements of  $d\sigma/dt$  at the ISR could indicate the need for the introduction of the BSW factor in the eikonal, more precise constraints on the form of  $W_{gg}(b)$  will only be available through further measurements of the high-energy behavior of the forward quantities studied here.<sup>52</sup> Actually, the current value of  $\sigma_{\text{tot}}$  at the  $S\bar{p}pS$  ( $61.9 \pm 1.5$  mb), lower than the preliminary results,<sup>2,54</sup> suits our model very well. A faster rise of  $\sigma_{\text{tot}}$  in the ISR-to- $S\bar{p}pS$  interval is not desirable in our picture since typical troublesome features of the earlier formulation of Ref. 17, such as a break in  $d\sigma/dt$  at small  $|t|$ , are recovered. Elastic scattering is probably the only available laboratory to study the gluon-gluon density overlap [ $W_{gg}(b)$ ] through such an analysis of shadow scattering from the inelastic channels.

Had we included scaling violations for  $F_{gg}(\tau)$  in Eq. (7), we believe that their influence would have been small. Their effect translates into a larger  $\text{Im}\chi$  near  $b=0$  and a

smaller  $\text{Im}\chi$  in the large- $b$  tail. We expect little effect in the region around  $b=1$  fm, and all the quantities which we are interested in depend sensitively only on this region of impact parameter.

We briefly compare our position among some of the currently successful models. The traditionally pure FE geometrical model promoted by Chou and Yang<sup>18,26,27</sup> has been recently revised by the same authors<sup>55</sup> (resulting in an “edgy” Chou-Yang model) and lost its pure FE character as well as some of its justification. This new formulation can be shown to be equivalent to a short-range expansion of the corresponding inelastic overlap function  $G_{\text{in}}$ .<sup>42</sup> The older Cheng, Walker, and Wu model,<sup>22</sup> revised by Chiu<sup>36</sup> [he adds the Regge parametrization of Eq. (14)], and the current version of the Bourrely, Soffer, and Wu model<sup>21</sup> are representatives of the pure FE type. Both use an asymptotic energy dependence “derived” from field theory<sup>36</sup> and no attempt is made to identify the role of any eventual proton constituent in either this energy dependence or the form factors chosen. There are also models which are not easily recognized to be of any familiar form. The new model of Chiu<sup>36</sup> (in which he modifies the Pomeron of Cheng, Walker, and Wu) is an example; he formulates his eikonal in  $t$  space. Our model is another example, but uses instead an eikonal constructed in  $b$  space. Among the various well-known models from the literature, that of Bourrely, Soffer, and Wu seems to be the one which reproduces well the widest set of data; as is obvious from the preceding sections, our model is of comparable usefulness.

A separation of the eikonal into two components as proposed here follows naturally from the presumed existence of elementary constituents of two different natures, matter and gauge fields, in the QCD-parton framework. The separation into an energy-independent and an energy-dependent term may be somewhat arbitrary, but we believe that having been able to relate the whole energy dependence of the forward quantities to the already successful phenomenological picture of the gluon, thought to be the active constituent of the proton in light particle central production<sup>14</sup> as well as, for example, in heavy flavor production,<sup>57</sup> makes it credible. The  $gg \rightarrow gg$  process has also recently been advocated<sup>58</sup> to be an important source of heavy quarks in large- $p_T$  jets at the  $S\bar{p}pS$ . This suggests that phenomenologically there is no difficulty in understanding the very different properties of soft and hard reactions at high energies. Schematically, the proposed new richer image of the gluon states that while hard reactions with small cross sections may be direct manifestations of all two-gluon fusion processes as in the usual models, soft central inelastic reactions may proceed through the competing indirect mechanism based on  $gg \rightarrow gg$  which was described in Ref. 14 and their shadow would explain the rise of  $\sigma_{\text{tot}}$ .

Our model is inscribed in the same current of thought as promoted by some authors<sup>15,59</sup> stating that soft physics may reveal much more about the structure of the proton than was previously believed. In other words, hard processes, the kingdom of perturbative QCD, are not the only grounds where the proton constituents leave footprints. In this sense our eikonal stands out in the crowd of com-

peting models since it is constructed on the basis of some known phenomenological properties of proton constituents.

## V. SUMMARY AND CONCLUSIONS

Our intention was to apply the language of the QCD-parton model to the description of important soft physics quantities like the total and differential elastic cross sections of the combined  $pp$  and  $p\bar{p}$  channels, assumed to be equivalent at high energies according to general asymptotic theorems. The impact-parameter formalism was used to describe a single crossing-even elastic amplitude. An eikonal function was built out of parton-model concepts; generalized distribution functions were assumed to factorize in the transverse-impact-parameter and the fractional-longitudinal-momentum variables. We separated the eikonal into two terms, a constant valence-quark contribution and a two-gluon-initiated term bearing the whole energy dependence at high energies, and constructed from an already existing model for the creation of light particles with low transverse momenta in the central region.

Density overlaps in  $b$  space were assumed for each of the two terms; this constitutes an important generalization over the model of Ref. 17. We made a simple assumption about the shape of the gluon-gluon density overlap and it was seen that this quantity controls the rate of rising of the total cross section. In our picture, all experimental data above the Fermilab range are well reproduced, but the Froissart bound is not saturated at very high energies.

Our two-component eikonal describes a compact proton (more so than in Ref. 17), but with a flexible shape granting it (without *a priori* assumptions) with nearly geometrical scaling characteristics in the ISR energy range and with some factorized eikonal features in the interval between the ISR and the  $S\bar{p}pS$ . The shape of  $W_{gg}(b)$  might become more precisely known in the future as the energy domain accessible to experiments is further extended. Our analysis provides information on the structure of the proton through shadow scattering of soft inelastic reactions.

For comparison with experimental data, our model can be treated at various levels of sophistication, depending on whether or not one requires a real part at lower energy or the absence of multiple diffraction dips in  $d\sigma/dt$  at large  $|t|$ . We showed how these finer details could be accounted for; we borrowed appropriate parametrizations from other existing models since those proved to be adequate and could hardly be improved upon. We would like to stress that, in its simplest formulation, our model has only five adjustable parameters, all physically well motivated, and that at high energy this basic "version 1" is well suited for detailed predictions of all relevant elastic diffraction quantities to be measured in the next decade(s) at projected accelerators.

*Note added in proof.* Two recent experimental publications may be of interest to the reader: M. Bozzo *et al.* (UA4 Collaboration), Phys. Lett. **155B**, 197 (1985); and N. Amos *et al.*, Nucl. Phys. B (to be published). In addition, the odderon contribution of Refs. 8 and 9 is further discussed in P. Gauron, B. Nicolescu, and E. Leader, Phys. Rev. Lett. **54**, 2656 (1985).

\*Present address: Laboratoire de Physique Nucléaire, Université de Montréal, Montréal, Québec, Canada, H3C 3J7.

<sup>1</sup>M. Bozzo *et al.* (UA4 Collaboration), Phys. Lett. **147B**, 392 (1984).

<sup>2</sup>G. Arnison *et al.* (UA1 Collaboration), Phys. Lett. **128B**, 336 (1983).

<sup>3</sup>J. Baumel, M. Feingold, and M. Moshe, Nucl. Phys. **B198**, 13 (1982); M. Baig, J. Bartels, and J. W. Dash, *ibid.* **B237**, 502 (1984); M. Baig, Report No. UAB-FT-119, Universitat Autònoma de Barcelona, Bellaterra (Barcelona), Spain, 1985 (unpublished).

<sup>4</sup>J. Dias de Deus and P. Kroll, J. Phys. G **9**, L81 (1983); Acta Phys. Pol. **B9**, 157 (1978); A. J. Buras and J. Dias de Deus, Nucl. Phys. **B71**, 481 (1974).

<sup>5</sup>M. Bozzo *et al.* (UA4 Collaboration), Phys. Lett. **147B**, 385 (1984).

<sup>6</sup>N. Amos *et al.* (R-211 Collaboration), Phys. Lett. **120B**, 460 (1983); **128B**, 343 (1983).

<sup>7</sup>A. Martin, Z. Phys. C **15**, 185 (1982); in *Proceedings of the 21st International Conference on High Energy Physics, Paris, 1982*, edited by P. Petiau and M. Porneuf [J. Phys. (Paris) Colloq. **43**, C3-164 (1982)]. In neglecting any odderon contribution we are endorsing "orthodoxy" as advocated by Martin, although we are aware that some authors (Refs. 8 and 9) see in the results of the R-210 Collaboration (Ref. 10) a small odderon contribution.

<sup>8</sup>B. Nicolescu, in *Proceedings of the 6th European Symposium on Nucleon-Antinucleon and Quark-Antiquark Interactions, Santiago de Compostela, Spain, 1982*, edited by C. Pajares (So-

ciudad Española de Física, Madrid 1983), p. 273; P. Gauron and B. Nicolescu, Phys. Lett. **124B**, 429 (1983); **143B**, 253 (1984).

<sup>9</sup>P. Gauron and B. Nicolescu, in  *$p\bar{p}$  Physics and the  $W$  Discovery*, proceedings of the Third Moriond Workshop, La Plagne-Savoie, 1983, edited by J. Tran Thanh Van (Editions Frontières, Gif-sur-Yvette, France, 1983), p. 107.

<sup>10</sup>M. Ambrosio *et al.* (R-210 Collaboration), Phys. Lett. **115B**, 495 (1982); G. Carboni *et al.*, Nucl. Phys. **B254**, 697 (1985).

<sup>11</sup>J. Fischer, Phys. Rep. **76**, 157 (1981); S. M. Roy, *ibid.* **5C**, 125 (1972); R. J. Eden, Rev. Mod. Phys. **43**, 15 (1971).

<sup>12</sup>C. Bourrely and A. Martin, in *Proceedings of the CERN-ECFA Workshop on the Feasibility of a Hadron Collider in the LEP Tunnel, Lausanne, 1984* (Report No. CERN 84-10), Vol. 1, p. 323; A. Martin, in *Proceedings of the Fourth Topical Workshop on  $p\bar{p}$  Collider Physics, Berne, 1984*, edited by H. Hänni and J. Schacher (Report No. CERN 84-09), p. 308; M. M. Block and R. N. Cahn, Phys. Lett. **120B**, 224 (1983).

<sup>13</sup>M. Froissart, Phys. Rev. **123**, 1053 (1961); A. Martin, Nuovo Cimento **42**, 930 (1966).

<sup>14</sup>P. L'Heureux and B. Margolis, Phys. Rev. D **28**, 242 (1983).

<sup>15</sup>K. Fiałkowski and W. Kittel, Rep. Prog. Phys. **46**, 1283 (1983).

<sup>16</sup>T. K. Gaisser, F. Halzen, and E. A. Paschos, Phys. Rev. D **15**, 2572 (1977); F. Halzen and S. Matsuda, *ibid.* **17**, 1344 (1978).

<sup>17</sup>Y. Afek, C. Leroy, B. Margolis, and P. Valin, Phys. Rev. Lett. **45**, 85 (1980).

<sup>18</sup>T. T. Chou and C. N. Yang, Phys. Rev. **170**, 1591 (1968).

<sup>19</sup>L. Durand and R. Lipes, Phys. Rev. Lett. **20**, 637 (1968); F.

- Hayot and U. P. Sukhatme, *Phys. Rev. D* **10**, 2183 (1974).
- <sup>20</sup>C. Bourrely, J. Soffer, and T. T. Wu, *Phys. Rev. D* **19**, 3249 (1979).
- <sup>21</sup>C. Bourrely, J. Soffer, and T. T. Wu, *Nucl. Phys.* **B247**, 15 (1984); *Phys. Rev. Lett.* **54**, 757 (1985).
- <sup>22</sup>H. Cheng, J. K. Walker, and T. T. Wu, *Phys. Lett.* **44B**, 97 (1973).
- <sup>23</sup>A. Martin, *Lett. Nuovo Cimento* **7**, 811 (1973).
- <sup>24</sup>R. Henzi and P. Valin, *Phys. Lett.* **149B**, 239 (1984).
- <sup>25</sup>J. B. Bronzan, G. L. Kane, and U. P. Sukhatme, *Phys. Lett.* **49B**, 272 (1974).
- <sup>26</sup>T. T. Chou and C. N. Yang, *Phys. Rev. D* **17**, 1889 (1978); **19**, 3268 (1979); *Phys. Rev. Lett.* **46**, 764 (1981).
- <sup>27</sup>T. T. Chou, T. T. Wu, and C. N. Yang, *Phys. Rev. D* **26**, 328 (1982).
- <sup>28</sup>U. Amaldi and K. R. Schubert, *Nucl. Phys.* **B166**, 301 (1980).
- <sup>29</sup>K. R. Schubert, in *Landolt-Börnstein Numerical Data and Functional Relationships in Science and Technology*, edited by H. Schopper (Springer, Berlin, 1980), New series, Group I, Vol. 9.
- <sup>30</sup>P. Valin, *Nucl. Phys.* **B218**, 215 (1983); *Z. Phys. C* **25**, 259 (1984).
- <sup>31</sup>M. Bozzo *et al.* (UA4 Collaboration), Report No. CERN/EP/1448R/GM/mk (unpublished); these results also appeared in G. Matthiae, rapporteur talk, in *Proceedings of the International Europhysics Conference on High Energy Physics, Brighton, 1983*, edited by J. Guy and C. Costain (Rutherford Appleton Laboratory, Chilton, Didcot, United Kingdom, 1984), p. 714.
- <sup>32</sup>M. Botje, Ph.D. thesis, University of Utrecht, 1984.
- <sup>33</sup>L. A. Fajardo *et al.*, *Phys. Rev. D* **24**, 46 (1981).
- <sup>34</sup>P. Carlson, in *Landolt-Börnstein Numerical Data and Functional Relationships in Science and Technology* (Ref. 29).
- <sup>35</sup>R. Henzi and P. Valin, *Phys. Lett.* **132B**, 443 (1983).
- <sup>36</sup>C. Chiu, *Phys. Lett.* **142B**, 309 (1984).
- <sup>37</sup>V. Franco, *Phys. Rev. D* **11**, 1837 (1975).
- <sup>38</sup>S. Sanielevici and P. Valin, *Phys. Rev. D* **29**, 52 (1984).
- <sup>39</sup>S. Sanielevici and P. Valin, *Phys. Rev. D* **32**, 586 (1985).
- <sup>40</sup>R. J. Glauber and J. Velasco, *Phys. Lett.* **147B**, 380 (1984).
- <sup>41</sup>See Refs. 24 and 35, and also R. Henzi and P. Valin, *Nucl. Phys.* **B148**, 513 (1979); contributed paper No. 701 to the 22nd International Conference on High Energy Physics, Leipzig, 1984 (unpublished); *Z. Phys. C* **27**, 351 (1985).
- <sup>42</sup>R. Henzi and P. Valin, *Phys. Lett.* (to be published).
- <sup>43</sup>A. Breakstone *et al.*, *Nucl. Phys.* **B248**, 253 (1984).
- <sup>44</sup>S. Erhan *et al.*, *Phys. Lett.* **152B**, 131 (1985).
- <sup>45</sup>A. Breakstone *et al.*, *Phys. Rev. Lett.* **54**, 2180 (1985).
- <sup>46</sup>M. M. Islam, T. Fearnley, and J. P. Guillaud, *Nuovo Cimento* **81A**, 737 (1984); G. W. Heines and M. M. Islam, *ibid.* **61A**, 149 (1981).
- <sup>47</sup>A. Donnachie and P. V. Landshoff, *Nucl. Phys.* **B231**, 189 (1984); *Phys. Lett.* **123B**, 345 (1983).
- <sup>48</sup>P. L'Heureux, Ph.D. thesis, McGill University, 1985; see Appendix F.
- <sup>49</sup>Experimental best fits to lower energy and ISR data by Bartel and Diddens (Ref. 50) and by Amaldi *et al.* (Ref. 51), of the form  $\sigma_{\text{tot}} \propto \log^{\beta} s$  with a constant  $\beta$ , included a  $\log^2 s$  and  $(\log s)^{2.1 \pm 0.1}$  term, respectively; adding the new  $S\bar{p}pS$  measurement, the UA4 Collaboration (Ref. 1) finds that the rise is "very close to a  $\log^2 s$  behavior."
- <sup>50</sup>W. Bartel and A. N. Diddens, CERN-NP Internal Report No. 73-4, 1973 (unpublished).
- <sup>51</sup>U. Amaldi *et al.*, *Phys. Lett.* **66B**, 390 (1977).
- <sup>52</sup>The  $pp$  total cross section estimated from a cosmic-ray experiment (Ref. 53),  $120 \pm 15$  mb at  $\sqrt{s} = 30$  TeV, is a bit higher than our prediction, but it should be noted that the extraction of this value is model dependent, as recognized by the authors.
- <sup>53</sup>R. M. Baltrusaitis *et al.*, *Phys. Rev. Lett.* **52**, 1380 (1984).
- <sup>54</sup>R. Battison *et al.* (UA4 Collaboration), *Phys. Lett.* **117B**, 126 (1982).
- <sup>55</sup>T. T. Chou and C. N. Yang, *Phys. Lett.* **128B**, 457 (1983).
- <sup>56</sup>H. Cheng and T. T. Wu, *Phys. Rev. Lett.* **24**, 1456 (1970), and references therein.
- <sup>57</sup>Among others, see Y. Afek, C. Leroy, and B. Margolis, *Phys. Rev. D* **23**, 760 (1981); **22**, 86 (1980); M. Glück and E. Reya, *Phys. Lett.* **79B**, 453 (1978); C. E. Carlson and R. Suaya, *Phys. Rev. D* **18**, 760 (1978); J. Babcock, D. Sivers, and S. Wolfram, *ibid.* **18**, 162 (1978); M. Glück, J. F. Owens, and E. Reya, *ibid.* **17**, 2324 (1978); L. M. Jones and H. W. Wyld, *ibid.* **17**, 1782 (1978); M. B. Einhorn and S. D. Ellis, *ibid.* **12**, 2007 (1975).
- <sup>58</sup>F. Halzen and P. Hoyer, *Phys. Lett.* **154B**, 324 (1985).
- <sup>59</sup>R. N. Cahn, in *Proceedings of DPF Workshop on  $\bar{p}p$  Options for the Super Collider, Chicago, 1984*, edited by J. E. Pilcher and A. R. White (Physics Department, University of Chicago, 1984), p. 117; R. C. Hwa, in *Partons in Soft Hadronic Processes*, proceedings of the Europhysics Conference, Erice, Italy, 1981, edited by R. T. van de Walle (World Scientific, Singapore, 1981).